



Showing research from Professor Shishido's laboratory,
Institute of Innovative Research, Tokyo Institute of
Technology, Tokyo, Japan.

Polymer-grafted ZnO nanorods enhance optical nonlinearity
of oligothiophene-doped liquid crystals

There is a growing interest in delivering new nonlinear optical (NLO) materials that can respond to low light intensities for the development of new-generation photonic devices. Liquid crystals (LCs) are commonly used NLO materials, but the higher sensitivity is required for photonic applications. The sensitivity of dye-doped LCs is enhanced by introducing polymer-grafted zinc oxide (ZnO) nanorods into the system, which allows the LCs to respond to lower threshold intensities.

As featured in:



See Shoichi Kubo,
Atsushi Shishido *et al.*,
Mater. Adv., 2022, **3**, 7531.

Cite this: *Mater. Adv.*, 2022,
3, 7531

Polymer-grafted ZnO nanorods enhance optical nonlinearity of oligothiophene-doped liquid crystals†

Jose Carlos Mejia,^{ab} Kohsuke Matsumoto,^{ab} Kaho Ogata,^{ab} Daisuke Taguchi,^{ab}
Kaho Nakano,^{ab} Shoichi Kubo *^{ab} and Atsushi Shishido *^{ab}

The photoinduced molecular reorientation of nonlinear optical materials is a promising approach to cause the nonlinear optical effect used for developing next-generation self-modulating and optical switching devices. Liquid crystals (LCs) attract much attention as nonlinear optical materials due to their large change in refractive index and high light sensitivity to induce molecular reorientation. However, the light intensity required to induce molecular reorientation of LC materials is high for optical devices requiring lower threshold intensities. Here, we report a system containing polymer-grafted ZnO nanorods in oligothiophene-doped host LCs able to induce molecular reorientation at lower threshold intensities shown by the formation of concentric diffraction rings. Incorporating 5 wt% of polymer-grafted ZnO nanorods in oligothiophene-doped host LCs significantly reduced the threshold intensity by 39% compared to pure oligothiophene-doped systems. This discovery will provide a new route to use inorganic nanorods in dye-doped host LCs as dopants to enhance the nonlinear optical effect at lower threshold intensities.

Received 29th June 2022,
Accepted 7th September 2022

DOI: 10.1039/d2ma00774f

rsc.li/materials-advances

1 Introduction

Nonlinear optical (NLO) materials, defined as materials that interact with light to produce a nonlinear response, are considered vital components for developing nano-scale optoelectronic and photonic devices.¹ Those materials are based on the NLO effect, where the optical properties of the material change when irradiated with a light source. NLO materials have significantly impacted laser technology due to their large NLO properties and fast NLO response for optoelectronic applications, such as optical switching,^{2,3} optical data storage,⁴⁻⁶ and optical limiters.⁷⁻⁹ Therefore, innovative NLO materials, such as nanorods,¹⁰ graphene oxide,^{11,12} and azo-functionalized nanoparticles,¹³ have been proposed and investigated for the development of future optoelectronic devices.

Liquid crystals (LCs) have been used as NLO materials due to their large molecular anisotropy and facile susceptibility to optical fields.¹⁴⁻¹⁸ Previous research reports showed that the

optical nonlinearity of LC molecules to an optical field was greatly enhanced by doping small amounts of dichroic dyes, such as derivatives from azobenzene,¹⁹⁻²² anthraquinone,²³⁻²⁶ and oligothiophene,^{27,28} into a host LC system. The dopants of dichroic dyes contribute to the total optical torque of LC molecules to respond to an optical electric field. As a result, the threshold intensity, where the molecular reorientation occurred in dye-doped host LCs, was drastically reduced compared with that in the pure host LC. However, the light intensity required to induce the molecular reorientation of dye-doped NLO materials is still high, preventing their usage in systems requiring lower threshold intensities.

We induced the molecular reorientation of oligothiophene dye-doped LCs at relatively low light intensities through polymer stabilization,²⁹⁻³¹ surface anchoring,³² hybrid alignment,³³ and assistance of an electric field.³⁴ In polymer-stabilized LCs (PSLCs), the threshold intensity was reduced by a factor of six compared to conventional homeotropic LCs.³⁵ The usage of PSLCs delivered optical limiters with a low threshold intensity, and the application of an electric field greatly enhanced their optical limiting threshold.³⁴ However, this low optical threshold intensity was only achieved by applying an electrical stimulus that can lead to a complex system. Therefore, a new NLO material that can lower the threshold intensity is necessary for developing optical switching, self-modulators, and holographic memory with simple systems.

In this study, we focused on doping inorganic nanomaterials in oligothiophene-dye doped LC systems to enhance the optical

^a Laboratory for Chemistry and Life Science, Institute of Innovative Research, Tokyo Institute of Technology, R1-12, 4259 Nagatsuta, Midori-ku, Yokohama 226-8503, Japan

^b Department of Chemical Science and Engineering, School of Materials and Chemical Technology, Tokyo Institute of Technology, 2-12-1 Ookayama, Meguro-ku, Tokyo 152-8552, Japan. E-mail: kubo@res.titech.ac.jp, ashishid@res.titech.ac.jp

† Electronic supplementary information (ESI) available. See DOI: <https://doi.org/10.1039/d2ma00774f>



nonlinearity of LC molecules. Inorganic nanomaterials, such as semiconductors, have been used as NLO materials due to their excellent NLO properties.^{36–38} The alignment of anisotropic nanomaterials enhances their NLO properties.¹⁰ Moreover, one-dimensional materials, such as nanorods, are attractive due to their elongated anisotropic shape and can facilitate the alignment of LC along the direction of the applied field. However, the miscibility of nanorods to host LCs remains an issue; inorganic nanorods tend to aggregate, thus, decreasing the material responsiveness.

Herein, we report a new, simple system of oligothiophene-doped LCs containing polymer-grafted zinc oxide (ZnO) nanorods, which shows lower threshold intensities compared to PSLC systems. The surface of ZnO nanorods was modified with a nematic LC polymer to enhance their miscibility with the host LC.³⁹ The ZnO nanorods were aligned parallel to the neighbouring host LC molecules due to the cooperative effect between the mesogens in the grafted polymers and the LC molecules.⁴⁰ The polymer-grafted nanorods in oligothiophene-doped LCs gave rise to a 39% reduction of threshold light intensity at 5 wt% of polymer-grafted ZnO nanorods. The results of this study can lead to future light-modulating materials and can be expanded to microscale optical devices and miniaturized lenses.

2 Experimental

2.1 Materials

The chemical structures of the constituent compounds used in this study are shown in Fig. 1. The ZnO nanorods were synthesized at a gram-scale with an average diameter of 7 nm and length of 50 nm, as reported elsewhere.⁴¹ In this report, poly{4-[4-(4-methoxyphenoxy)carbonyl]phenoxy}butyl methacrylate, PMA(4OPB), showing a nematic LC phase, was used as the grafted polymer. The PMA(4OPB)-grafted ZnO nanorods, henceforth termed polymer-grafted nanorods, were synthesized using our previously reported procedure (Fig. S1, ESI†).³⁹



Fig. 1 Chemical structures of the materials used in this study.

A nematic host LC, 5CB (4-cyano-4'-pentylbiphenyl), was provided from Merck Ltd, Tokyo, Japan. The oligothiophene guest-dye molecule, TR5 (5,5''-bis-(5-butyl-2-thienylethynyl)-2,2':5',2''-terthiophene), was synthesized as reported previously.⁴² Tetrahydrofuran (THF with stabilizer, 99.5%) and 2-propanol (IPA, 99.5%) were purchased from FUJIFILM Wako Pure Chemical Corp., Osaka, Japan.

2.2 Methods

2.2.1 Sample preparation. The compositions of the constituent compounds are shown in Table 1. First, a 0.10 M TR5 in a THF solution was prepared and doped into 5CB, followed by solvent evaporation in a vacuum desiccator to prepare a mixture of TR5-doped 5CB. The composition ratio of 5CB to TR5 was 99.9 to 0.1 mol%. Second, the synthesized polymer-grafted nanorods were added to a THF solution and ultrasonicated until the nanorods were fully dispersed in the solvent. The suspension containing the polymer-grafted nanorods was added into the mixture of TR5-doped 5CB, followed by ultrasonication and stirring for 30 min and 1 h, respectively. The solvent was evaporated overnight in a vacuum desiccator. The name of each sample of TR5-doped LCs containing polymer-grafted ZnO nanorods was labelled as LCZ-X, where X is the weight fraction of polymer-grafted nanorods to TR5-doped 5CB.

2.2.2 LC cell preparation. Two commercially available glass substrates (2.5 cm × 2.5 cm) were ultrasonically cleaned with IPA for 30 min. Subsequently, the glass substrates were treated with a UV-ozone cleaner for 10 min, then a precursor solution (SE-3210, Nissan Chemical Corporation, Tokyo, Japan) was deposited on the glass substrate to form a uniform homeotropic alignment layer through spin-coating. After spin-coating, the glass substrates were treated at 120 °C for 2 h to yield surface-treated glass substrates that can align LC molecules homeotropically. Next, the glass cells were fabricated by sandwiching two surface-treated glass substrates with 100 μm-thick polyimide tapes. The sample mixtures containing various weight fractions of polymer-grafted nanorods in TR5-doped 5CB were injected into the LC cell by capillary forces at 70 °C and cooled down to room temperature at a scanning rate of 2 °C min⁻¹.

2.3 Characterization techniques

The polymer-grafted nanorods were subjected to thermogravimetric analysis (TGA, Shimadzu Corp., DTA-60, Kyoto, Japan), conducted in an air atmosphere at a heating rate of

Table 1 The compositions of LCZ-X

Sample	Compositions (wt%)	
	TR5/5CB ^a	ZnO-PMA(4OPB)
LCZ-0	100	0
LCZ-1	99	1
LCZ-2	98	2
LCZ-5	95	5

^a The guest-dye molecule, TR5, is doped into 5CB at a dye concentration of 0.1 mol%.



10 °C min⁻¹, to determine the mass of the grafted polymer on the nanorod (Fig. S2, ESI†). The thermodynamic properties of the samples were determined by differential scanning calorimetry (DSC, Hitachi High-Tech Corp., DSC7000X, Tokyo, Japan). The heating and cooling cycles were repeated three times to verify the reproducibility at a scanning rate of 1 °C min⁻¹, and the third scan of the heating curve was reported. The initial molecular alignment in the LC cell was observed with a polarized optical microscope (POM, BX50, Olympus Corp., Tokyo, Japan). The conoscopic image was taken with an interference filter at 546 nm, where the sample does not have any absorbance. A polarized ultraviolet-visible absorption spectrophotometer (UV-vis, V-670, JASCO Corp., Hachioji, Japan) equipped with a rotary polarizer was used to confirm the homeotropic alignment of the TR5 molecules in the LC cell.

2.4 Optical setup

The self-diffraction ring formation was investigated to evaluate the photoinduced molecular reorientation behaviour of the TR5-doped LCs containing polymer-grafted nanorods. The optical setup used in this research is shown in Fig. 2. A linearly polarized beam with a wavelength of 488 nm was used as the pump laser (EXLSR-488C-200-CDRH, Spectra-Physics, MKS Instruments, Inc., Milpitas, CA, USA). The beam diameter before L1 was 800 μm and then expanded to 1.9 mm by the lenses, L1 and L2. Spatial filtering of the laser beam was performed with a pinhole ($\phi = 50 \mu\text{m}$) and the lens, L3. The LC cell was placed at the focal point ($f = 15 \text{ cm}$) of the lens, L4. The light intensity was controlled using a variable neutral density filter (VND). The incident laser beam power W_0 on the LC cell was calculated by taking the ratio of the beam power split by a non-polarizing cube beam splitter. The light intensity at the irradiation spot was defined as $I = W_0/\pi r^2$, where r is the radius of the laser beam at the focal point of L4. The laser beam diameter at the focal point was 50 μm. The LC cell was exposed to the laser beam with sufficiently high intensity giving rise to the formation of concentric diffraction ring patterns observed on a white screen placed behind the LC cell. The concentric

diffraction rings were counted visually at each light intensity. The molecular reorientation threshold was defined as the lowest light intensity to induce one self-diffraction ring observed with a beam profiler (BGP-USB-SP620, Ophir-Spiricon LLC., North Logan, UT, USA).

3 Results and discussion

3.1 Miscibility of polymer-grafted nanorods with oligothiophene-doped host LC

The miscibility of polymer-grafted nanorods with TR5-doped 5CB was confirmed using DSC measurements (Fig. S3, ESI†). The nematic LC polymer, PMA(4OPB), which is the polymer grafted to the nanorods in this study, shows a nematic (N)-to-isotropic (I) phase transition temperature (T_{NI}) at 103 °C according to a previous report.³⁹ However, no endothermic peaks were observed at the T_{NI} of PMA(4OPB), indicating the miscibility of the polymer-grafted nanorods in the TR5-doped host LC. In addition, the N-I phase transition enthalpies (ΔH_{NI}) of TR5-doped LCs containing polymer-grafted nanorods were calculated (Table 2). The enthalpy peak at the T_{NI} became smaller with increasing weight fractions of polymer-grafted nanorods, which indicates that the nanorods disordered the neighbouring LC molecules. The phase transition behaviour of the samples was observed with a POM equipped with a hot stage (Fig. S4, ESI†). The samples were placed on a clean glass slide covered with a cover glass and heated from 35 °C to 50 °C at a scanning rate of 1 °C min⁻¹ to evaluate the phase transition behaviour. The samples containing polymer-grafted nanorods showed a broader phase transition temperature range. This indicates that the N phase of TR5-doped 5CB was thermally broadened by the addition of polymer-grafted nanorods.²⁹ The degree of stabilization was enhanced as the weight fraction of polymer-grafted nanorods increased.

3.2 Alignment of oligothiophene-doped host LC containing polymer-grafted nanorods

The LC cells fabricated by injecting LCZ-X by capillary forces showed a uniform and optically transparent yellow colour over the entire area (top photographs in Fig. 3a-d) due to the colour of TR5. The conoscopic POM images of the LC cells exhibited a clear isogyre (middle photographs in Fig. 3a-d). These observations suggest the homeotropic alignment of TR5-doped 5CB



Fig. 2 Schematic diagram of the optical setup for self-diffraction measurements. VND, variable neutral density filter; Sh, shutter; M, mirror; L1, plane concave lens ($f = -8 \text{ cm}$); L2, plane convex lens ($f = 20 \text{ cm}$); L3, plane convex lens ($f = 7.5 \text{ cm}$); PH, pinhole; I, iris; PM, power meter; B/S, beam splitter; P, polarizer; L4, bi-convex lens ($f = 15 \text{ cm}$); S, LC cell sample. The beam diameter before L4 was 1.9 mm. The sample was placed at a focal point of L4 where the diameter of the beam was 50 μm.

Table 2 Characteristics of TR5-doped LCs containing polymer-grafted nanorods

Sample	Enthalpy,		Absorbance at 488 ^b nm	Threshold Intensity (W cm ⁻²)	Max. # of Rings
	T_{NI} ^a (°C)	ΔH_{NI} ^a (kJ mol ⁻¹)			
LCZ-0	35.3	0.49	0.166	19.7	24
LCZ-1	35.5	0.66	0.178	15.8	25
LCZ-2	35.1	0.55	0.178	14.6	26
LCZ-5	34.5	0.54	0.180	12.0	27

^a Determined by DSC (heating, 3rd scan). ^b Determined by polarized UV-vis absorption spectra.





Fig. 3 Orientation of TR5-doped host LC containing polymer-grafted nanorods. Photograph (top), conoscopic (middle), and orthoscopic (bottom) polarized optical micrographs observed with a 20 \times objective lens of LC cells containing LCZ samples at the concentrations of 0 (a), 1 (b), 2 (c), and 5 (d) wt%. The scale bar is 50 μm . (e) Polarized UV-vis absorption spectra for LCZ-X. (f) Schematic representation of TR5-doped LCs containing polymer-grafted nanorods.

and polymer-grafted nanorods in the LC cell. The homeotropic alignment of polymer-grafted nanorods may be due to the cooperative effect of the LCs.^{39,40} The orthoscopic POM images of the LC cells showed great dispersion of polymer-grafted nanorods in TR5-doped LCs (bottom photographs in Fig. 3a-d). The homeotropic alignment of the TR5 was also confirmed by polarized UV-vis spectroscopy (Fig. 3e), where the sample injection direction was defined as the parallel direction. The parallel and perpendicular absorption spectra in the wavelength range of 5CB and TR5 molecules were the same, independent of the polarization direction (Fig. S5, ESI[†]). The maximum absorbance at 433 nm was increased with the addition of polymer-grafted nanorods. The increment in maximum absorbance suggests that polymer-grafted nanorods disordered the orientation of neighbouring 5CB and TR5 molecules, which is also evident by the DSC measurement. The absorbances at 488 nm of all samples are shown in Table 2. A schematic representation of the molecular orientation in the LC cell is shown in Fig. 3f.

3.3 Optical nonlinearity of TR5-doped LCs containing polymer-grafted nanorods

Based on the NLO effect, the photoinduced molecular reorientation of LC molecules exhibits a lucid dependence on the incident light intensity. Previous reports showed that the threshold intensity to induce the NLO effect in oligothiophene-doped LC systems was lowered by polymer stabilization.^{29,35} Therefore, the photoinduced molecular reorientation of the prepared polymer-grafted nanorods in oligothiophene-doped LC systems was examined by irradiation with a laser beam at a wavelength of



Fig. 4 Principle of the self-diffraction ring formation. (a) No diffraction ring is observed for low light intensities. (b) Diffraction rings are observed for high light intensities through self-focusing and self-phase modulation, which are arising from the nonlinear molecular reorientation.

488 nm. The diffraction ring patterns of different weight fractions of polymer-grafted nanorods at various incident light intensities are shown in Fig. S6 (ESI[†]). The formation of concentric rings is a typical NLO effect based on the change of refractive index resulting from the molecular reorientation of anisotropic molecules.^{19,43,44} The shape of the transmitted laser beam remained intact (*i.e.*, no formation of diffraction rings) below the threshold intensity of photoinduced molecular reorientation. Concentric diffraction rings began to appear above the threshold intensity due to self-focusing and self-phase modulation (Fig. 4). The number of diffraction rings increased with higher incident light intensities (Fig. 5).

TR5-doped 5CB without nanorods (LCZ-0) had a threshold intensity of 19.7 W cm^{-2} . The addition of polymer-grafted nanorods into the system lowered the threshold intensity. For LCZ-1, the threshold intensity decreased to 15.8 W cm^{-2} , *i.e.*, 20% lower than LCZ-0. Increasing the weight fractions of polymer-grafted nanorods lowered the threshold intensity even more to 14.6 and 12.0 W cm^{-2} for LCZ-2 and LCZ-5, respectively. This finding indicates that the addition of polymer-grafted nanorods can enhance the optical nonlinearity of TR5-doped host LCs.

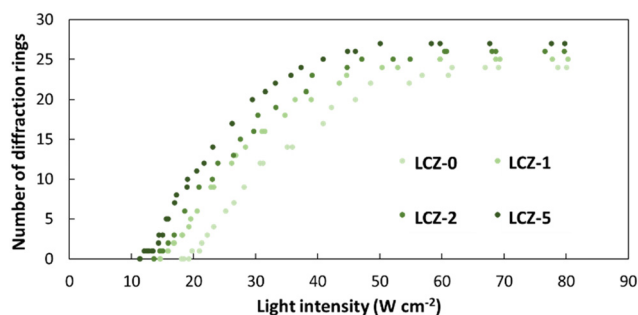


Fig. 5 Number of diffraction rings as a function of light intensity for LCZ-X.





Fig. 6 Number of diffraction rings as a function of light intensity for TR5-doped LCs with (LCZ-5) and without (LCZ-0) polymer-grafted nanorods, and with homopolymer (LCP-5).

LCZ samples with polymer-grafted nanorods are analogous to PSLCs as both systems contain a polymer. Previous studies suggested that PSLC systems with a polymer concentration of 10 mol% reduced the threshold intensity by 85%.³⁵ The LCZ-5 system used in our study decreased the threshold intensity by 39%. The weight fraction of polymer-grafted nanorods cannot be increased to match the PSLC system containing a polymer concentration of 10 mol% because polymer-grafted nanorods at high-weight fractions tend to phase separate with the host LC. As a result, to compare PSLC systems with LC systems containing polymer-grafted nanorods, the polymer concentration of both systems needs to be comparable. The amount of the polymer grafted on the surface of the nanorod was measured by TGA, and the weight fractions of the nanorod and grafted polymer were calculated as 0.413 and 0.587, respectively.

To better understand whether the nanorods or the homopolymer of PMA(4OPB) enhanced the optical nonlinearity, TR5-doped LCs containing a homopolymer, PMA(4OPB), were prepared. The TR5-doped LCs containing a homopolymer at different polymer concentrations, termed LCP-1, LCP-2, and LCP-5, were used so that the polymer concentrations match with those of LCZ-1, LCZ-2, and LCZ-5, respectively (Table S1, ESI†). For example, LCZ-1 and LCP-1 have the same polymer concentration of PMA(4OPB). Glass cells of TR5-doped LCs containing the homopolymer also showed a uniform and optically transparent yellow colour (top photographs in Fig. S7, ESI†). The homeotropic alignment of the TR5-doped LCs containing the homopolymer was confirmed from conoscopic POM images and UV-vis absorption spectra (middle photographs and bottom graphs in Fig. S7, ESI†, respectively). The optical nonlinearity of the TR5-doped LCs with the homopolymer was evaluated similarly to those with polymer-grafted nanorods. The formation of self-diffraction rings with light intensity is shown in Fig. S8 (ESI†), and the results are summarized in Table S2 (ESI†). LCZ-5 and LCP-5 showed similar absorbance at 488 nm and were used to compare the threshold intensity reduction with the TR5-doped host LC containing neither polymer-grafted nanorods nor homopolymer (Fig. 6). The threshold intensities of LCZ-5 and LCP-5 are 12.0 and 15.2 W cm^{-2} with a 39% and 22.8% threshold intensity reduction, respectively. The results indicate that incorporating

nanorods has a higher impact on reducing the threshold intensity than the homopolymer.

The most common approach to investigate the reason behind this reduction of threshold intensity is to understand the order parameter of the molecules. The disordering of the molecules was estimated by measuring the order parameter of TR5 in homogeneously (in-plane) aligned LCZ and LCP samples (Fig. S9, ESI†). The results suggest that incorporating 1 wt% of polymer-grafted nanorods caused a 21% reduction in the order parameter of TR5 compared to the sample with no polymer-grafted nanorods. It is doable to state that the decrease in threshold intensity was caused by the disordering of LC and TR5 molecules in the LC cell, which makes facile parallel alignment along the polarization direction of the optical electric field of the laser beam (Fig. S10, ESI†). In the case of the samples containing only the homopolymer, there was almost no molecular disordering caused by the homopolymers, but the threshold intensity was reduced. The reason for this is that the homopolymer weakens the surface anchoring in the LC cells, which allows molecules to align at lower threshold intensities.²⁹ In short, incorporating polymer-grafted nanorods caused a slight disordering of LC and TR5 molecules and weakened the forces from the surface anchoring in the LC cells. In addition, the ZnO nanorods might influence the elastic constant of the LCs that can cause the LC molecules to be more susceptible to a molecular reorientation when irradiated with a polarized light source. In the future, more experiments will be conducted to fully understand the role of ZnO nanorods in the dye-doped LCs, in terms of elastic constant, dielectric anisotropy, and rotational viscosity, to cause the NLO effect at lower threshold intensities.

Conclusions

In summary, we have demonstrated that incorporating polymer-grafted nanorods in oligothiophene-doped host LCs lowered the threshold intensities to induce a molecular reorientation compared with oligothiophene-doped LCs alone. The photoinduced molecular reorientation of oligothiophene-doped host LCs containing polymer-grafted nanorods was confirmed by observing the formation of concentric diffraction rings that appeared on the screen behind the sample due to the self-focusing and self-phase modulation. The threshold intensity decreased by 20% when 1 wt% of polymer-grafted nanorods were added into oligothiophene-doped LCs. As the weight fraction of the polymer-grafted nanorods was increased to 5%, the threshold intensity was reduced by 39%. The results were compared to PSLCs containing the homopolymer, and ZnO nanorods were confirmed to have a higher NLO effect than LCs containing the homopolymer alone. The results of this study concluded that the incorporation of polymer-grafted nanorods stabilized the N phase of LCs while causing a slight disordering to their orientation, all of which made the LCs more susceptible to molecularly align parallel to the polarization direction of an optical electric field at lower light



intensities. This investigation will lead to the development of nano optoelectronic devices and photonic materials that can induce such NLO effects at lower light threshold intensities.

Author contributions

J. C. M., K. M., S. K., and A. S. conceived and planned the nonlinear optical experiments; S. K. and A. S. supervised the project; J. C. M. synthesized the polymer-grafted nanorods, fabricated all the LC samples, measured the optical properties, and analysed the experimental data; K. M. helped with the measurement of optical properties; K. O., D. T., and K. N. helped with the synthesis of polymer-grafted nanorods; J. C. M. took the lead in writing the manuscript with the support of K. M., S. K., and A. S. All authors have given approval to the final version of the manuscript.

Conflicts of interest

The authors declare no competing financial interest.

Acknowledgements

This research was supported by Grant-in-Aid for Scientific Research on Innovative Areas “Molecular Engine” (JSPS KAKENHI Grant number JP18H05422), Grant-in-Aid for Scientific Research(B) (JSPS KAKENHI Grant number 22H02128), and JST CREST Grant Number JPMJCR1814. This work was performed under the Cooperative Research Program of “Network Joint Research Center for Materials and Devices.” This work was performed under the Research Program of “Dynamic Alliance for Open Innovation Bridging Human, Environment and Materials” and “Crossover Alliance to Create the Future with People, Intelligence and Materials” in “Network Joint Research Center for Materials and Devices.” The authors are grateful to Katsumi Suda for kindly measuring the TGA of our sample. The authors are also grateful to Kiyoshi Kanie from Tohoku University for his assistance in the XRF analysis. The authors thank all the members of the Shishido-Kubo group at the Tokyo Institute of Technology for their kind assistance and discussions.

References

- 1 P. Günter, *Nonlinear optical effects and materials*, Springer, 2012.
- 2 U. A. Hrozhyk, S. V. Serak, N. V. Tabiryan, L. Hoke, D. M. Steeves and B. R. Kimball, *Opt. Express*, 2010, **18**, 8697–8704.
- 3 F. Castet, V. Rodriguez, J.-L. Pozzo, L. Ducasse, A. Plaquet and B. Champagne, *Acc. Chem. Res.*, 2013, **46**, 2656–2665.
- 4 A. S. Matharu, S. Jeeva and P. S. Ramanujam, *Chem. Soc. Rev.*, 2007, **36**, 1868.
- 5 I. C. Khoo, M.-Y. Shih, M. V. Wood, B. D. Guenther, P. H. Chen, F. Simoni, S. S. Slussarenko, O. Francescangeli and L. Lucchetti, *Proc. IEEE*, 1999, **87**, 1897–1911.
- 6 A. Shishido, *Polym. J.*, 2010, **42**, 525–533.
- 7 Z. Guo, F. Du, D. Ren, Y. Chen, J. Zheng, Z. Liu and J. Tian, *J. Mater. Chem.*, 2006, **16**, 3021–3030.
- 8 Y.-X. Zhang and Y.-H. Wang, *RSC Adv.*, 2017, **7**, 45129–45144.
- 9 R. Udayabhaskar, M. S. Ollakkan and B. Karthikeyan, *Appl. Phys. Lett.*, 2014, **104**, 013107.
- 10 H. Zhang, Z. Hu, Z. Ma, M. Gecevičius, G. Dong, S. Zhou and J. Qiu, *ACS Appl. Mater. Interfaces*, 2016, **8**, 2048–2053.
- 11 N. Dalir, S. Javadian and Z. Dehghani, *J. Mol. Liq.*, 2017, **244**, 103–109.
- 12 G.-K. Lim, Z.-L. Chen, J. Clark, R. G. Goh, W.-H. Ng, H.-W. Tan, R. H. Friend, P. K. Ho and L.-L. Chua, *Nat. Photonics*, 2011, **5**, 554–560.
- 13 A. Miniewicz, J. Girones, P. Karpinski, B. Mossety-Leszczak, H. Galina and M. Dutkiewicz, *J. Mater. Chem. C*, 2014, **2**, 432–440.
- 14 N. V. Tabiryan and B. Y. Zel'Dovich, *Mol. Cryst. Liq. Cryst.*, 1980, **62**, 237–250.
- 15 N. V. Tabiryan, A. V. Sukhov and B. Y. Zel'Dovich, *Mol. Cryst. Liq. Cryst.*, 1986, **136**, 1–139.
- 16 G. Barbero and F. Simoni, *Appl. Phys. Lett.*, 1982, **41**, 504–506.
- 17 G. Barbero, F. Simoni and P. Aiello, *J. Appl. Phys.*, 1984, **55**, 304–311.
- 18 F. Simoni and R. Bartolino, *Opt. Commun.*, 1985, **53**, 210–212.
- 19 I. A. Budagovsky, V. N. Ochkin, S. A. Shvetsov, A. S. Zolot'ko, A. Y. Bobrovsky, N. I. Boiko and V. P. Shibaev, *Phys. Rev. E*, 2017, **95**, 052705.
- 20 L. Lucchetti, M. Di Fabrizio, O. Francescangeli and F. Simoni, *Opt. Commun.*, 2004, **233**, 417–424.
- 21 I. Khoo, S. Slussarenko, B. Guenther, M.-Y. Shih, P. Chen and M. Wood, *Opt. Lett.*, 1998, **23**, 253–255.
- 22 L. Lucchetti, M. Gentili, F. Simoni, S. Pavliuchenko, S. Subota and V. Reshetnyak, *Phys. Rev. E: Stat., Nonlinear, Soft Matter Phys.*, 2008, **78**, 061706.
- 23 I. Jánossy, A. D. Lloyd and B. S. Wherrett, *Mol. Cryst. Liq. Cryst. (1969–1991)*, 1990, **179**, 1–12.
- 24 I. Jánossy and A. D. Lloyd, *Mol. Cryst. Liq. Cryst.*, 1991, **203**, 77–84.
- 25 I. Janossy and T. Kosa, *Opt. Lett.*, 1992, **17**, 1183–1185.
- 26 L. Marrucci, *Liq. Cryst. Today*, 2002, **11**, 6–33.
- 27 T. Kosa, P. Palfy-Muhoray, H. Zhang and T. Ikeda, *Mol. Cryst. Liq. Cryst.*, 2004, **421**, 107–115.
- 28 M. Yaegashi, A. Shishido, T. Shiono and T. Ikeda, *Chem. Mater.*, 2005, **17**, 4304–4309.
- 29 Y. Aihara, M. Kinoshita, J. Wang, J.-I. Mamiya, A. Priimagi and A. Shishido, *Adv. Opt. Mater.*, 2013, **1**, 787–791.
- 30 K. Matsumoto, K. Usui, N. Akamatsu and A. Shishido, *J. Photopolym. Sci. Technol.*, 2020, **33**, 77–80.
- 31 K. Matsumoto, K. Usui, N. Akamatsu and A. Shishido, *Mol. Cryst. Liq. Cryst.*, 2020, **713**, 46–54.
- 32 K. Usui, E. Katayama, J. Wang, K. Hisano, N. Akamatsu and A. Shishido, *Polym. J.*, 2017, **49**, 209–214.
- 33 J. Wang, Y. Aihara, M. Kinoshita, J.-I. Mamiya, A. Priimagi and A. Shishido, *Sci. Rep.*, 2015, **5**, 9890.



- 34 K. Usui, K. Matsumoto, E. Katayama, N. Akamatsu and A. Shishido, *ACS Appl. Mater. Interfaces*, 2021, **13**, 23049–23056.
- 35 J. Wang, Y. Aihara, M. Kinoshita and A. Shishido, *Opt. Mater. Express*, 2015, **5**, 538–548.
- 36 L. W. Tutt and T. F. Boggess, *Prog. Quantum Electron.*, 1993, **17**, 299–338.
- 37 Y. Williams, K. Chan, J. H. Park, I. C. Khoo, B. Lewis and T. E. Mallouk, *Liq. Cryst. IX*, 2005, **5936**, 225–230.
- 38 I. C. Khoo, K. Chen and Y. Z. Williams, *IEEE J. Sel. Top. Quantum Electron.*, 2006, **12**, 443–450.
- 39 S. Kubo, R. Taguchi, S. Hadano, M. Narita, O. Watanabe, T. Iyoda and M. Nakagawa, *ACS Appl. Mater. Interfaces*, 2014, **6**, 811–818.
- 40 K. Ogata, K. Matsumoto, Y. Kobayashi, S. Kubo and A. Shishido, *Molecules*, 2022, **27**, 689.
- 41 S. Kubo and M. Nakagawa, *Chem. Lett.*, 2012, **41**, 1137–1138.
- 42 H. Zhang, S. Shiino, A. Shishido, A. Kanazawa, O. Tsutsumi, T. Shiono and T. Ikeda, *Adv. Mater.*, 2000, **12**, 1336–1339.
- 43 S. D. Durbin, S. M. Arakelian and Y. R. Shen, *Phys. Rev. Lett.*, 1981, **47**, 1411–1414.
- 44 S. Durbin, S. Arakelian and Y. Shen, *Opt. Lett.*, 1981, **6**, 411–413.

